

Evaluation of corticostriatal oscillations as a monitoring biomarker for ethanol and sweet/fat food consumption in rats

Running title: corticostriatal oscillations as biomarkers

Lucas L. Dwiel, Angela M. Henricks, Jiang Gui, and Wilder T. Doucette*

Lucas Dwiel PhD Department of Psychiatry, Geisel School of Medicine at Dartmouth

Angela Henricks PhD Department of Psychology, Washington State University

Jiang Gui PhD Geisel School of Medicine at Dartmouth

*Corresponding Author

Wilder Doucette MD PhD Department of Psychiatry, Geisel School of Medicine at Dartmouth

One Medical Center Drive, Lebanon NH 03756-0001

Tel: 603-650-8597

Wilder.t.doucette@dartmouth.edu

Abstract

The majority of individuals that abuse addictive substances tend to struggle with more than one, therefore optimal therapeutic strategies should generalize across substances. Although closed-loop interventions (neuromodulatory and mobile-device based) are emerging for the treatment of substance use, they require monitoring biomarkers that detect when an individual is about to use, or is using, a substance. Based on our prior work we hypothesized that corticostriatal oscillations could be used to detect the consumption of 10% ethanol (EtOH) or sweet-fat food (SF) from all other behaviors using the same oscillatory features. We conditioned Sprague-Dawley rats to consume EtOH or SF and then recorded corticostriatal local field potentials during consumption of the two substances and their naturalistic controls (i.e., water/house-chow). We used lasso and simple logistic regressions to determine which corticostriatal features were predictive of consuming each substance alone or combined. Although both substances were detectable ($\text{EtOH} = 0.81 \pm 0.01$ and $\text{SF} = 0.68 \pm 0.01$; area under the receiver operator characteristic curve), the models did not detect consumption of the other substance ($\text{SF} \rightarrow \text{EtOH} = 0.43 \pm 0.01$ and $\text{EtOH} \rightarrow \text{SF} = 0.49 \pm 0.01$) and models built using both datasets only detected the consumption of EtOH ($\text{gen} \rightarrow \text{EtOH} = 0.63 \pm 0.04$ and $\text{gen} \rightarrow \text{SF} = 0.5 \pm 0.04$). These results suggest

that a model that generalizes across substances is not feasible. However, due to the low consumption of EtOH, the difficulty in differentiating EtOH from water, and the inability to detect imminent EtOH consumption it may be that EtOH is not salient enough in rats to be a useful model substance in this context.

Introduction

The maladaptive use of more than one substance (e.g., tobacco, alcohol and palatable food), is highly prevalent in the US [1,2] with over 70% of US adults with a substance use disorder reporting the use of multiple substances [3] and up to 50% of individuals with eating disorders also struggle with other substances [4]. Importantly, polysubstance abuse is associated with poorer treatment outcomes and higher mortality rates [2] - highlighting the need to develop treatments that can target the misuse of more than one substance.

Emerging treatments targeting the brain networks that regulate these appetitive behaviors (e.g., deep brain stimulation; DBS) have demonstrated therapeutic potential across substances [5–7] and palatable food [8,9]. For emerging interventions that directly modulate the activity of brain networks and are implanted or wearable, there is an opportunity to minimize side effects by only triggering an intervention during critical time windows immediately preceding or during maladaptive behaviors [10,11]. For example, a closed-loop DBS system for epilepsy detects neural activity that predicts an imminent seizure and triggers stimulation to reduce the likelihood of seizure onset [12,13].

Closed-loop approaches are well suited for problems that occur in discrete moments in time, like substance use or binge eating. For a closed-loop treatment approach to work in brain

stimulation or mobile-device delivered interventions, monitoring biomarkers with adequate temporal resolution, sensitivity, and specificity are required to trigger an effective intervention. These biomarkers allow interventions to be implemented immediately preceding or during maladaptive behavior. Although these biomarkers could come from external sources that, for example, identify proximity to established cues/contexts that trigger maladaptive behavior, we have shown that neural oscillations, in rodents, can predict the imminent onset of binge eating behavior [14]. Similar prediction models have been used to trigger DBS of the nucleus accumbens (NAc) to reduce the amount of palatable food consumed in a rodent model of binge eating [11] and this approach is being implemented in a clinical trial for loss-of-control eating in patients with treatment resistant obesity.

As a central node within the brain networks controlling appetitive behavior, the NAc plays a well-established role in encoding the pursuit and receipt of rewarding substances [15,16] and is known to be a strong moderator of hedonic food and ethanol intake [17,18]. We previously demonstrated that neural oscillations – i.e., local field potentials (LFPs) – recorded from the NAc can be used to differentiate epochs of binge eating from all other behavior and predict if feeding is about to occur [14], and we hypothesized that the same would be possible for rats conditioned to drink 10% ethanol (EtOH) [19,20]. We also hypothesized that a single predictive model could use LFPs to differentiate both EtOH and sweet-fat food (SF) consumption from all other behaviors including water and house chow consumption. To test these hypotheses, we constructed predictive models built from data during feeding or drinking sessions to detect SF or EtOH consumption. We also tested these models on the other dataset (e.g., detecting EtOH drinking using the model built from feeding data). Finally, we built and tested models on the drinking and feeding datasets combined to determine if a generalized model could classify EtOH or SF consumption from all other behavior.

Materials and Methods

Three cohorts of 60-day old Sprague-Dawley rats (Charles River, Shrewsbury, MA) were individually housed using a reverse 12-hour light/dark schedule with house chow (HC) and water (H_2O) available *ad libitum*. We conditioned the first cohort ($n = 12$ males) to binge sweet-fat food (SF). We conditioned the second cohort ($n = 5$ males and 4 females) to drink 10% ethanol (EtOH). To address sex differences in EtOH drinking, we increased our sample size by conditioning a third cohort ($n = 5$ males and 5 females) to drink EtOH after they served as a control group in an unrelated experiment [20]. We carried out all experiments in accordance with the NIH Guide for the Care and Use of Laboratory Animals (NIH Publications no. 80-23, revised in 1996) and approved by the Institutional Animal Care and Use Committee at Dartmouth College.

General methods

Electrode Implantation

Surgery and electrode construction was done similarly to previous experiments [21]. We targeted the first cohort's (feeding) electrodes to the bilateral NAc shell (AP 1.2 mm; ML ± 1 ; and DV -7.6 mm relative to bregma) and the NAc core (AP 1.2 mm; ML ± 2.4 mm; and DV -7.6 mm relative to bregma). We targeted the second and third cohort's (drinking) electrodes to the bilateral rat medial prefrontal cortex (infralimbic cortex - AP 3.4 mm; ML ± 0.75 mm; and DV -5 mm relative to bregma) and NAc shell.

Behavioral measures

Following recovery from surgery (~1 week), we gave rats intermittent access to either: 1) SF (Figure 1A), containing 4.6 kcal/g and 19% protein, 36.2% carbohydrates, and 44.8% fat by calories (Teklad Diets 06415, South Easton, MA); or 2) EtOH (Figure 1B), as described previously [14]. Figure 1C and D illustrates the percent of rats actively consuming SF or EtOH over the course of a limited access session. We weighed the SF and EtOH before and after all sessions to calculate the amount consumed during the session (Figure 1C and D insets, respectively). After 16-20 sessions the rats consumed a stable and significant amount of SF ($54\pm12\%$ of their daily caloric intake; mean \pm 1 standard deviation). On average, rats drank 0.49 ± 0.38 g/kg of EtOH (mean \pm 1 standard deviation) corresponding to a BAC of about 0.01-0.02% [22].

Local field potential recording and processing

We tethered rats in an 18"x12"x24" chamber through a commutator to a Plexon data acquisition system (Plexon, Plano, TX) with time-synchronized video for offline analysis. We manually scored videos that were time-locked to the neural data to identify time intervals of food or liquid consumption using Plexon Cineplex software (Figure 1A and B). We used custom code written for Matlab R2019a for all LFP signal processing as previously reported [14] and used the following frequency bands: delta = 1-4 Hz, theta = 5-10 Hz, alpha = 11-14 Hz, beta = 15-30 Hz, low gamma = 45-65 Hz, and high gamma = 70-90 Hz. To compare recordings across rats and across days, we normalized power per frequency band as the percent of total power of the signal from 1 to 90 Hz and normalized coherence per frequency band and channel pair as the z-score from the average coherence within each channel pair.

Verification of electrode placement

We euthanized rats at the end of the experiment using CO₂. For histologic verification of electrode placement we removed the brains, flash froze in 2-methylbutane, sectioned with a cryostat, mounted on slides, and stained with thionine [21]. No rats required exclusion based on electrode location [20,23].

Model building overview

We aligned non-overlapping 5-second bins of LFP data to fit within one of four possible behavioral categories: “consuming” for SF or EtOH, “control” for house chow (HC) or H₂O, “pre-consumption” for SF or EtOH, or “not” for all other behavior (i.e., not “consuming”, not “control”, and not “pre-consumption”). We defined pre-consumption bins as those occurring up to 1 minute prior to consumption initiation and we discarded them if they overlapped with a previous consuming bin (Figure 1E and F). We included H₂O and HC data in our model training to control for potential noise generated due to the physical act of consuming (e.g., chewing and swallowing) as well as signals that are not specific to the consumption of SF or EtOH, but are features of eating and drinking in general. We used the same number of bins from each rat (weighting bins as needed) and balanced the number of bins for each group (e.g., consuming vs. not+control) to prevent the creation of a majority classifier.

We evaluated model performances using naïve data (excluded from model building) to calculate the classification probabilities with the Matlab function *predict()*, constructing a receiver operator characteristic (ROC) curve and calculating the area under the ROC curve (AUROC) with the function *perfcurve()*. We built all models using multiple iterations of random data selection for model building and testing and so the reported performances are the average of the 100 iterations with 95% confidence intervals. We used statistical inference by permutation to assess

the by-chance accuracy of the models. Specifically, we used Monte Carlo sampling to shuffle the assignment of predictors (i.e., LFP features) and outcome variables (e.g., consuming vs. not+control) from the same data sets described above and we present these average AUROC values with corresponding 95% confidence intervals alongside the real (i.e., unshuffled) model performances.

We used the lasso algorithm for all models except when we built simple logistic models using each LFP feature individually to quantify the amount of predictive information of each feature alone and to see if the same features were similarly predictive across datasets.

Identifying predictive LFP features

To quantify how much predictive information was contained within each LFP feature, we also built the consuming vs. not+control and pre-consumption vs. not+control models using each LFP feature by itself with 100 iterations of sub-sampling and weighting. We then directly compared the average AUROC of each feature on either the feeding or the drinking dataset. We represented the direction of the correlation between the LFP features and consumption by giving the AUROCs a sign (e.g., if increased beta power from the right NAc shell correlated with drinking EtOH, then the AUC would be positive). In this way, we can visualize features with an AUROC above 0.5 on a 2-dimensional Cartesian plot such that features that correlate with the behavior in the same direction across feeding and drinking models will lie in quadrants I and III.

Building models for specific substances – consuming vs. not+control

First, we analyzed the feeding dataset and drinking dataset separately to determine if LFPs during consuming SF or EtOH were differentiable from LFPs during consuming control (i.e., HC or H₂O) and all other behaviors.

From each rat, we used 40 total bins: 20 consuming bins (i.e., consumption of SF or EtOH), 10 control bins (i.e., HC or H₂O), and 10 not bins (i.e., all other behaviors). To minimize overfitting we: 1) held out a random 20% of the data for a test set (80/20); or 2) held out each rat as a test set (leave-one-out; LOO). For the 80/20 split, we repeated the sub-sampling and weighting process 100 times. For LOO, we repeated the sub-sampling/weighting 100 times for each of the held out rats. We also split the test set into consuming vs. naturalistic control and consuming vs. not to assess if the models were actually differentiating the consumption of EtOH or sweet-fat food from their naturalistic controls. We first built models using all LFP features and then, to ensure that performances were directly comparable, using only the shared 18 features from bilateral NAc shell.

Sex differences in predictors of EtOH drinking

We used the third cohort (n = 4 males and 5 females) to determine if there are any sex differences in the drinking data. From each rat, we used 20 bins of LFP data: 10 drinking EtOH, 5 drinking water, and 5 not drinking anything. For each sex, we built 500 models by 100 iterations of sub-sampling and weighting for each rat left out for testing. We then tested these models on the left-out rats of the same sex or each of the rats from the opposite sex to determine if models performed better within sex.

Building models that generalize across substances

To determine if we could build a model to detect times of consumption of either SF or EtOH, we combined the 18 LFP features shared between the two substance specific cohorts; 12 power features and 6 coherence features from bilateral NAc shell. We then created training and test sets using both 80/20 and LOO. For LOO, we had eighty-one training/test sets representing all

possible iterations that included a rat from each cohort (i.e., feeding and drinking) in the left-out test data.

Pre-consumption vs. not

For greater temporal resolution, we calculated LFP features using a 5-second window with 80% overlap (i.e., ‘advancing’ the window by 1 second), up to a minute before feeding or drinking began. We built the models using 20 bins from each rat: 10 pre-consumption bins that immediately preceded consumption (i.e., the first 5 seconds before consumption) and 10 not bins at least 1 minute away from consumption (Figure 1E and F). We used 100 iterations of holding out 20% of the data for the test set. Pre-consumption vs. not models used all LFP features from each cohort (i.e., feeding and drinking), providing 216 features, with 198 features unique to each dataset in addition to the 18 shared features mentioned above.

Visualizing LFP feature changes around consuming epochs

To visualize the dynamics of features of interest, we used the normalized feature values from all recordings around both feeding and drinking, up to 1 minute before and after consumption occurred. Due to the differences in the average bout length of consumption between feeding and drinking, with feeding bouts being longer than drinking bouts, we used 9 seconds of data at the beginning and end of feeding while we used 5 seconds for drinking.

Results

All LFP features predicting consuming vs. not

Feeding

Figure 2 (A, D, and E) illustrates that LFPs recorded from the NAc core and shell are capable of classifying brain activity recorded during consuming SF from all other behaviors including consuming HC. The 80/20 models classified consuming SF with an average AUROC of 0.83 ± 0.01 and a permuted AUROC of 0.51 ± 0.02 (Figure 2A). When we used LOO the AUROC for SF vs. not+control classification was 0.68 ± 0.01 and the corresponding permuted performance was 0.50 ± 0.01 (Figure 2D). The performance of the models on differentiating SF vs. chow or SF vs. not are nearly identical (0.68 ± 0.01 and 0.69 ± 0.01 ; Figure 2D). While the distribution of AUROCs for the 80/20 models were normally distributed (Figure 2A inset), the distribution of the LOO model performances have a bimodal distribution (Figure 2E) which was due to poor performance predicting behavior in one rat.

Drinking

Figure 2 (A, B and C) demonstrate that LFPs recorded from the NAc shell and rat mPFC are capable of classifying brain activity recorded during consuming EtOH from all other behavior including consuming H₂O. The 80/20 models classified consuming EtOH with an average AUROC of 0.84 ± 0.01 and permuted AUROC of 0.50 ± 0.02 (Figure 2A). When we used LOO the AUROC for EtOH vs. not+control classification was 0.81 ± 0.01 and the corresponding permuted performance was 0.51 ± 0.01 (Figure 2B). We show the distribution of AUROCs for the 80/20 and

LOO models in Figure 2A inset and 2C respectively. Unlike feeding, the performance of these models on EtOH vs. H₂O is lower than on EtOH vs. not (0.64±0.01 vs. 0.89±0.01; Figure 2B).

Sex differences in predictors of EtOH drinking

Regardless of which sex the models were built from, when they were tested on male rats they performed similarly (M→M = 0.81±0.02 vs. F→M = 0.80±0.004; Figure 2F). Whereas, when models were built and tested on female rats they did slightly better than when built on male rats (F→F = 0.88±0.01 vs. M→F = 0.83±0.06; Figure 2F). Overall, the LFP feature differences between consuming EtOH vs. not+control likely have slightly higher signal to noise in females compared to males (i.e., a model built with female data does nearly as well as a model built with male data when predicting male drinking while a model built from male data does not do as well at predicting female drinking as a model built from female data), but the feature identities and direction of change is similar between sexes.

Common LFP features predicting consumption vs. not+control

Feeding

Figure 3 (A and E) illustrates that LFPs recorded from the bilateral NAc shell are capable of classifying consuming SF from all other behavior including consuming HC. The 80/20 models classified consuming SF with an average AUROC of 0.77±0.01 and permuted models performed with an average AUROC of 0.51±0.02 (Figure 3A). When we used LOO the real

AUROC for consuming SF vs. not+control classification was 0.76 ± 0.01 and the corresponding permuted performance was 0.50 ± 0.01 (Figure 3E).

Drinking

Figure 3 (A and E) illustrates that LFPs recorded from the bilateral NAc shell are capable of classifying brain activity recorded during consuming EtOH from all other behavior including consuming H₂O. The 80/20 models classified consuming EtOH with an average AUROC of 0.75 ± 0.01 and permuted models performed with an average AUROC of 0.52 ± 0.02 (Figure 3A). When LOO approach was used the real AUROC for consuming EtOH vs. not+control classification was 0.72 ± 0.01 and the corresponding permuted performance was 0.49 ± 0.02 (Figure 3E).

Testing models across datasets

When either 80/20 or LOO approaches were evaluated on data of the other substance type the performances dropped to chance level (i.e., AUROC = 0.5) or below (Figure 3B and F). The “drink→feed” (built on drinking data and tested on feeding data) had an average AUROC of 0.51 ± 0.01 (80/20) and 0.49 ± 0.01 (LOO). The “feed→drink” performances had an average AUROC of 0.43 ± 0.01 (80/20) and 0.43 ± 0.01 (LOO). While we could classify either feeding or drinking behavior, these models did not generalize across substance types. To determine if we could build a single model capable of predicting both SF and EtOH consumption from all other behavior we constructed models from the combination of both datasets.

Testing models built to generalize across substances

When we built models using LFPs from both datasets (feeding and drinking) they differentiated consumption of either SF or EtOH from all other behavior including HC and H₂O consumption (Figure 3C and G). The performance of models predicting SF+EtOH vs. not+control had an average AUROC of 0.68±0.01 for 80/20 with a corresponding permuted performance of 0.5±0.01. When we tested these generalized models on the individual datasets (e.g., gen → feed) the AUROC on the feeding data was 0.54±0.01 and 0.63±0.01 on the drinking data (Figure 3C). Using the LOO approach, the performance of models predicting SF+EtOH vs. not+control had an average AUROC of 0.66±0.03 with a corresponding permuted performance of 0.52±0.03. When we tested these generalized models on the individual datasets the AUROC on the feeding data was 0.5±0.04 and 0.63±0.04 on the drinking data (Figure 3G).

To explore why the generalized models performed poorly compared to the substance specific models and performed better on one dataset than the other (i.e., drink > feed) we determined the performance of single feature logistic models built and tested on drinking or feeding data (Figure 3D and H). We found that many single LFP feature models perform better than chance for both substance types but that the direction of change around consumption was frequently in the opposite direction (quadrants II and IV in Figure 3D and H). Very few features changed in the same direction around consumption of EtOH and SF as indicated by the small number of features in quadrants I and III.

All LFP features predicting pre-consumption vs. not

LFPs recorded immediately preceding consumption identified intervals of imminent SF consumption, but were unable to identify imminent EtOH consumption.

Feeding

The performance of models built to identify the 5 seconds immediately preceding SF consumption versus not (see Supplemental: Pre-consumption vs. not models) outperformed permuted models and demonstrated declining performance with temporal distance from the start of SF consumption (Figure 4A). While performance of the pre-feeding model proximal to consumption approached performance levels of the consumption vs. not model (horizontal green bar at 0 sec), performance approached chance level 42.5 seconds prior to feeding initiation. To visualize how the model performance increases approaching feeding initiation related to predictive LFP features, we visualized an individual LFP feature around SF consumption (Figure 4B). The horizontal black line indicates the 'not' average feature value and the dashed green horizontal line the SF consumption average feature value. In this example, delta frequency (i.e, 1-4 Hz) coherence between the left and right NAc shell drops leading up to the consumption of SF food. To confirm that LFP features used to predict imminent SF consumption were likely capturing the same LFP changes that manifest during consumption, we determined the performance of single feature logistic models built and tested on SF consumption or pre-consumption data sets. We found that many single LFP feature models perform better than chance for both model types and that the direction of change frequently occurred in the same direction (quadrants I and III in Figure 4C).

Drinking

The performance of models built to identify the 5 seconds immediately preceding consuming EtOH versus not (see Supplemental: Pre-consumption vs. not) did not meaningfully outperform permuted models and did not vary with temporal distance from the start of EtOH consumption (Figure 4D). Performance of the pre-drinking model tested just prior to EtOH consumption performed far worse than the consumption versus not model (horizontal red bar). As shown for the feeding data, we visualized a top feature from EtOH pre-consumption models around intervals of consuming EtOH (Figure 4E). The horizontal black line indicates the not average feature value and the dashed red horizontal line the EtOH consumption average feature value. In this example, high gamma power in the right medial prefrontal cortex (infralimbic cortex) shows no ramping changes leading up to EtOH consumption and instead undergoes a rapid change upon initiation of EtOH consumption. The performance of single feature logistic models built and tested on EtOH consumption or pre-consumption data sets showed that many single LFP features performed better than chance for the consuming EtOH models, but few performed well in pre-consumption models with most AUROCs hovering around ± 0.5 (Figure 4F).

Discussion

These results suggest that neural oscillations recorded from the NAc shell are predictive of when the consumption of EtOH or highly palatable food is occurring compared to all other behaviors, including the consumption of less palatable food or water, respectively. Models built to predict consumption of both substances reveal that the features of NAc shell oscillations containing information about drinking are mostly distinct from those that are predictive of feeding. However, with the right combination of these features, we can predict the consumption of either substance, but with poorer performance than models including data from corticostriatal

brain regions (i.e., NAc core and mPFC). Further, LFP features recorded from the NAc shell change in advance of palatable food consumption allowing for the prediction of imminent consumption, but similar changes in advance of EtOH consumption were not detectable in the EtOH drinking paradigm using NAc shell and mPFC oscillations.

Overall, this work demonstrates that systems-level brain activity (i.e., neural oscillations) can identify periods of consumption of at least two distinct rewarding substances from all other behaviors in real-time. The demonstration that brain oscillations can identify when addiction-related behavior is occurring (i.e., serve as a monitoring biomarker) is a critical step in the development of next generation closed-loop and adaptive treatment systems that could alleviate the symptoms of appetitive disorders like loss-of-control eating or alcohol drinking.

Implications for Substance Use Disorders

A shared feature of addictive substances, like alcohol, is that they activate common brain regions – particularly the NAc – in ways that bias these networks to select behavior supporting continued substance use [24]. Though not traditionally considered an “addictive substance”, highly palatable food activates these networks similarly to abused substances [25]. The NAc is known to play a role in the intake of hedonically desirable food [27,28] and this may contribute to our ability to detect food consumption. Further, rats will readily consume palatable foods [29] while EtOH is naturally aversive [30] which may explain why it was harder to tell EtOH apart from H₂O than SF from HC. Although it is promising that NAc oscillations can identify both feeding and alcohol drinking, an interesting next step would be to extend these findings to other traditional drugs of abuse (e.g., cocaine, opioids, or nicotine). Doing so would help determine if other abused substances share the same neural activity patterns that are associated with SF or EtOH consumption.

Why can't imminent EtOH consumption be predicted?

Although we could detect imminent consumption of SF, we could not predict imminent EtOH consumption. When we plotted features used by the model through time around the behaviors of interest, we found that the temporal dynamics of these features were radically different around feeding versus around EtOH drinking. Many of the features had slow changes leading up to the beginning of feeding and then would slowly return back to the average during all other behavior after SF feeding ended; however, in the case of EtOH drinking, the top features exhibited rapid shifts that were outside of the temporal resolution of the models we used to predict imminent behavior. In order to predict imminent EtOH consumption, we propose that either a smaller time window should be used for analysis (and thus limiting one to using high frequency features, like high gamma) or other brain regions should be explored for more predictive features. Given that rats have a natural taste aversion to EtOH and must be conditioned in some way to drink it [31–33], the corticostriatal network may be minimally engaged and generates an insufficient signal to predict imminent EtOH drinking. Although using a limited access paradigm did induce the rats to escalate EtOH consumption, the volumes were relatively small (Figure 1D, inset). Future work to predict EtOH drinking in rats should use a forced EtOH dependence, which is known to increase the amount and salience of EtOH consumed through negative reinforcement.

Sex differences in EtOH drinking

Although, there are known sex differences in EtOH drinking [20,34,35], our generalized models indicate that information contained within neural oscillations can predict EtOH drinking in a sex independent manner. Our sex specific EtOH models predicting consuming vs. not also demonstrate that a large amount of information generalizes across sexes (Figure 2A and B).

Whether significant sex differences exist in the data or not, representation of all possible biological variables in a data set strengthens the generalizability of these types of predictive models.

Limitations

A limitation of these data is that the relationships between neural patterns and behavior are correlational; this is sufficient for monitoring biomarkers, but provides little insight into the potential of identified features to serve as treatment targets. A vital next step would be to manipulate the LFP features used to predict consuming food or EtOH and see if the behavior also changes, as has been demonstrated in Parkinson's disease with beta frequency oscillations [36–38]. Second, our feeding data was a re-analysis of a previously published dataset [14] that did not include female rats, thus preventing an assessment of sex specific LFP features of feeding. Future work would need to address the generalizability of these models to female rats as we demonstrated here for the EtOH models. Third, the feeding models contained no LFP recordings from frontal brain regions that would be accessible with non-invasive recording approaches (e.g., EEG). The presented EtOH data suggest that there is a significant amount of overlapping information contained within NAc and infralimbic cortex LFPs. We anticipate that a similar relationship exists for feeding as frontal regions are heavily involved in the regulation of feeding behavior [17]. Lastly, although we are using relatively few rats (cohort 1: n = 12; cohort 2: n = 9; and cohort 3: n = 10), our sample sizes ultimately come from the 5-second windows of clean data, meaning we consistently had 100s of samples to build models.

Conclusion

The consumption of ethanol and sweet-fat food is reflected in neural oscillations recorded in the NAc allowing the prediction of when either behavior is occurring compared to all other behavior, including naturalistic controls (ie., drinking water or eating less palatable house chow).

Nonetheless, most individual LFP features correlated better to one behavior over the other.

Future work will need to determine if the consumption of other addictive substances, like nicotine or opioids, could be incorporated into a polysubstance model. Overall, these data support the ongoing evaluation of a polysubstance monitoring biomarker derived from corticostriatal oscillations.

Funding and Disclosures

This work was supported by funds from an NIAAA training grant (F31AA027441; LD), the Hitchcock Foundation (AH), a NIDA T32 training grant (DA037202; AH), an LRP grant from NIH NCATS (KL2TR001088; WD), and a K08 grant from NIMH (1K08MH117347-01A1; WD). The authors have no competing financial interests to report.

References

1. Hedden SL. Behavioral Health Trends in the United States: Results from the 2014 National Survey on Drug Use and Health. 2015.
2. Crumy EA, O'Neal TJ, Baskin BM, Ferguson SM. One Is Not Enough: Understanding and Modeling Polysubstance Use. *Front Neurosci.* 2020;0. doi:10.3389/fnins.2020.00569
3. McCabe SE, West BT, Jutkiewicz EM, Boyd CJ. Multiple DSM-5 substance use disorders: A national study of US adults. *Hum Psychopharmacol.* 2017;32. doi:10.1002/hup.2625
4. Food for thought: Substance abuse and eating disorders. PsycEXTRA Dataset. 2003.

doi:10.1037/e541112013-001

5. Luigjes J, van den Brink W, Feenstra M, van den Munckhof P, Schuurman PR, Schippers R, et al. Deep brain stimulation in addiction: a review of potential brain targets. *Mol Psychiatry*. 2012;17: 572–583.
6. Guercio LA, Wimmer ME, Schmidt HD, Swinford-Jackson SE, Pierce RC, Vassoler FM. Deep brain stimulation of the infralimbic cortex attenuates cocaine priming-induced reinstatement of drug seeking. *Brain Res*. 2020;1746: 147011.
7. Pierce RC, Vassoler FM. Deep brain stimulation for the treatment of addiction: basic and clinical studies and potential mechanisms of action. *Psychopharmacology*. 2013;229: 487–491.
8. Kumar R, Simpson CV, Froelich CA, Baughman BC, Gienapp AJ, Sillay KA. Obesity and deep brain stimulation: an overview. *Ann Neurosci*. 2015;22: 181–188.
9. Lee DJ, Elias GJB, Lozano AM. Neuromodulation for the treatment of eating disorders and obesity. *Ther Adv Psychopharmacol*. 2018;8: 73–92.
10. Wu H, Adler S, Azagury DE, Bohon C, Safer DL, Barbosa DAN, et al. Brain-Responsive Neurostimulation for Loss of Control Eating: Early Feasibility Study. *Neurosurgery*. 2020. doi:10.1093/neuros/nyaa300
11. Wu H, Miller KJ, Blumenfeld Z, Williams NR, Ravikumar VK, Lee KE, et al. Closing the loop on impulsivity via nucleus accumbens delta-band activity in mice and man. *Proc Natl Acad Sci U S A*. 2018;115: 192–197.
12. Nair DR, Laxer KD, Weber PB, Murro AM, Park YD, Barkley GL, et al. Nine-year prospective efficacy and safety of brain-responsive neurostimulation for focal epilepsy. *Neurology*. 2020;95: e1244–e1256.
13. Morrell MJ, RNS System in Epilepsy Study Group. Responsive cortical stimulation for the treatment of medically intractable partial epilepsy. *Neurology*. 2011;77: 1295–1304.
14. Dwiel LL, Khokhar JY, Connerney MA, Green AI, Doucette WT. Finding the balance between model complexity and performance: Using ventral striatal oscillations to classify feeding behavior in rats. *PLoS Comput Biol*. 2019;15: e1006838.
15. Koob GF, Volkow ND. Neurocircuitry of Addiction. *Neuropsychopharmacology*. 2010. pp. 217–238. doi:10.1038/npp.2009.110
16. The neurobiology of drug addiction. *The Journal of Neuropsychiatry and Clinical Neurosciences*. 1997. pp. 482–497. doi:10.1176/jnp.9.3.482
17. Saper CB, Chou TC, Elmquist JK. The need to feed: homeostatic and hedonic control of eating. *Neuron*. 2002;36: 199–211.
18. Imperato A, Di Chiara G. Preferential stimulation of dopamine release in the nucleus accumbens of freely moving rats by ethanol. *J Pharmacol Exp Ther*. 1986;239: 219–228.
19. Henricks AM, Dwiel LL, Deveau NH, Simon AA, Ruiz-Jaquez MJ, Green AI, et al. Corticostratial Oscillations Predict High vs. Low Drinkers in a Rat Model of Limited Access

- Alcohol Consumption. *Front Syst Neurosci.* 2019;13: 35.
- 20. Henricks AM, Sullivan EDK, Dwiel LL, Keus KM, Adner ED, Green AI, et al. Sex differences in the ability of corticostriatal oscillations to predict rodent alcohol consumption. *Biol Sex Differ.* 2019;10: 61.
 - 21. Doucette WT, Khokhar JY, Green AI. Nucleus accumbens deep brain stimulation in a rat model of binge eating. *Transl Psychiatry.* 2015;5: e695.
 - 22. Li J, Zou Y, Ye J-H. Low frequency electroacupuncture selectively decreases voluntarily ethanol intake in rats. *Brain Res Bull.* 2011;86: 428–434.
 - 23. Doucette WT, Dwiel L, Boyce JE, Simon AA, Khokhar JY, Green AI. Machine Learning Based Classification of Deep Brain Stimulation Outcomes in a Rat Model of Binge Eating Using Ventral Striatal Oscillations. *Front Psychiatry.* 2018;9: 336.
 - 24. Koob GF, Volkow ND. Neurobiology of addiction: a neurocircuitry analysis. *Lancet Psychiatry.* 2016;3: 760–773.
 - 25. Balleine BW. Neural bases of food-seeking: affect, arousal and reward in corticostriatolimbic circuits. *Physiol Behav.* 2005;86: 717–730.
 - 26. Begg DP, Woods SC. Hedonic and homeostatic overlap following fat ingestion. *Cell metabolism.* 2013. pp. 459–460.
 - 27. Zhang M, Kelley A. Intake of saccharin, salt, and ethanol solutions is increased by infusion of a mu opioid agonist into the nucleus accumbens. *Psychopharmacology.* 2002. pp. 415–423. doi:10.1007/s00213-001-0932-y
 - 28. Zhang M, Kelley AE. Enhanced intake of high-fat food following striatal mu-opioid stimulation: microinjection mapping and Fos expression. *Neuroscience.* 2000. pp. 267–277. doi:10.1016/s0306-4522(00)00198-6
 - 29. Corwin RL, Avena NM, Boggiano MM. Feeding and reward: perspectives from three rat models of binge eating. *Physiol Behav.* 2011;104: 87–97.
 - 30. Cicero TJ. A Critique of Animal Analogues of Alcoholism. *Biochemistry and Pharmacology of Ethanol.* 1979. pp. 533–560. doi:10.1007/978-1-4684-3450-7_27
 - 31. Priddy BM, Carmack SA, Thomas LC, Vendruscolo JCM, Koob GF, Vendruscolo LF. Sex, strain, and estrous cycle influences on alcohol drinking in rats. *Pharmacol Biochem Behav.* 2017;152: 61–67.
 - 32. Wise RA. Voluntary ethanol intake in rats following exposure to ethanol on various schedules. *Psychopharmacologia.* 1973;29: 203–210.
 - 33. Wayner MJ, Greenberg I, Tartaglione R, Nolley D, Fraley S, Cott A. A new factor affecting the consumption of ethyl alcohol and other sapid fluids. *Physiol Behav.* 1972;8: 345–362.
 - 34. Nieto SJ, Kosten TA. Female Sprague-Dawley rats display greater appetitive and consummatory responses to alcohol. *Behav Brain Res.* 2017;327: 155–161.
 - 35. Lancaster FE, Spiegel KS. Sex differences in pattern of drinking. *Alcohol.* 1992;9: 415–420.

36. Kehnemouyi YM, Wilkins KB, Anidi CM, Anderson RW, Afzal MF, Bronte-Stewart HM. Modulation of beta bursts in subthalamic sensorimotor circuits predicts improvement in bradykinesia. *Brain*. 2021;144: 473–486.
37. Chen Y, Gong C, Tian Y, Orlov N, Zhang J, Guo Y, et al. Neuromodulation effects of deep brain stimulation on beta rhythm: A longitudinal local field potential study. *Brain Stimul*. 2020;13: 1784–1792.
38. Yin Z, Zhu G, Zhao B, Bai Y, Jiang Y, Neumann W-J, et al. Local field potentials in Parkinson's disease: A frequency-based review. *Neurobiol Dis*. 2021;155: 105372.

Figure Legends

Figure 1. Naturalistic feeding and drinking behavior synchronized to local field potential recording to build models predicting consuming 10% ethanol (EtOH) or sweet-fat food (SF). Panel **A** depicts the experimental setup in which we recorded video and local field potentials while rats had free access to either SF or house chow (HC) within the recording chamber. Panel **B** depicts a similar setup for drinking behavior except that rats could have access to water (H_2O) and EtOH simultaneously. Panels **C** and **D** illustrate the percent of rats engaged in SF or EtOH consumption through normalized session time and the amount of SF or EtOH consumed inset. Panels **E** and **F** depict how local field potentials are divided into 5 second bins that are aligned within hand-scored behavioral intervals (green and blue) and calculated behavioral intervals (light green and light blue). We used this segmentation of the data to construct models as outlined in model types (below **E** and **F**).

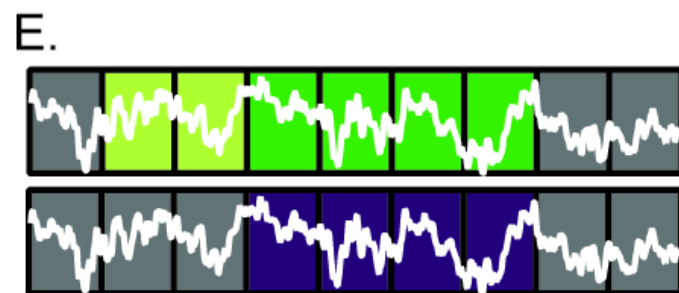
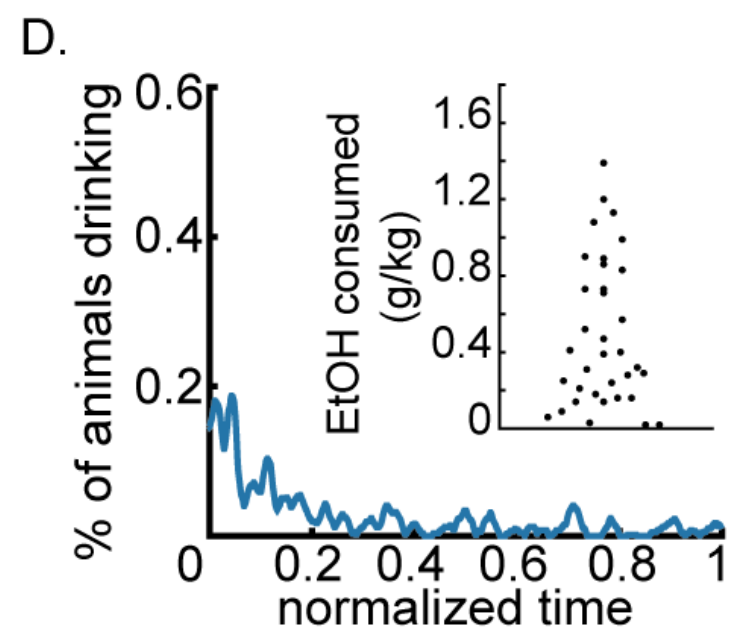
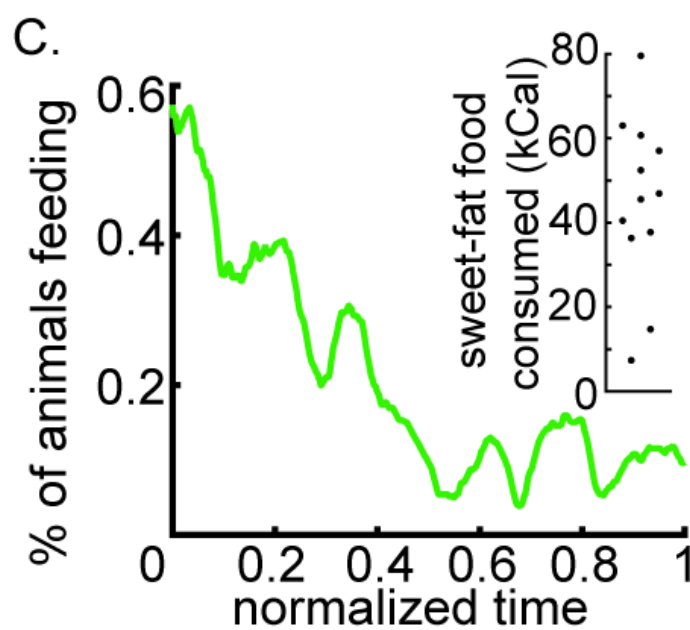
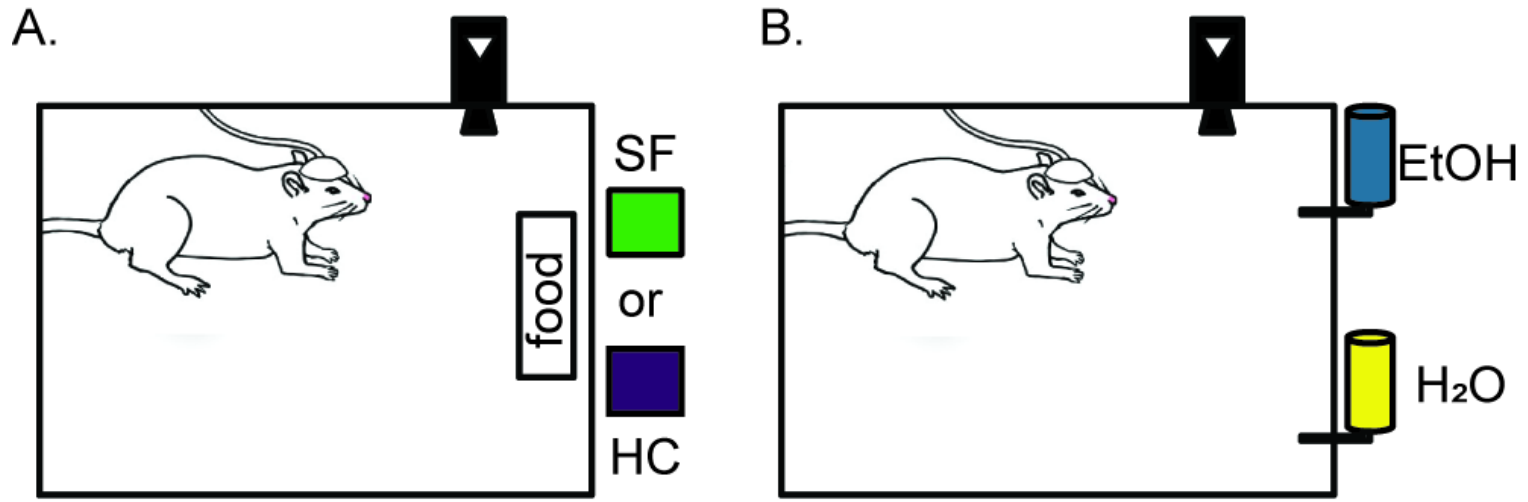
Figure 2. Local field potentials recorded from rat medial pre-frontal cortex and ventral striatal regions predict when rats are consuming sweet-fat food (SF) and 10% ethanol (EtOH). Panel **A** depicts the performance (i.e., receiver operator characteristic curve; ROC) of models predicting SF consumption (green) or EtOH (blue) versus all other behavior including the consumption of house chow (HC) or water (H_2O) respectively. The ROC curves illustrate how the true positive rate (TPR) varies in relation to the false positive rate (FPR). The average area under the ROC (AUROC) is listed for each curve \pm 95% confidence intervals (AUROC = 1 is a perfect model and 0.5 represents chance). The “perm” curves and AUROC values describe the performance of corresponding models built and tested on permutations of the real data. The inset distribution illustrates how the AUROC varied across different iterations of model building (80% of data) and testing (20% of data). Panel **B** illustrates the performance of drinking models in which we left-out (leave one out; LOO) whole rats during the model building process and tested models on the left out rats. We also show the performance of the model on EtOH vs. H_2O and EtOH vs. not

separately. The distributions of the model performances of the EtOH vs. all other behaviors and permuted data summarized in **B** are depicted in **C**. Panel **D** illustrates the performance of feeding LOO models with the performance of SF vs. HC and SF vs. not shown separately. The distributions of model performances of the SF vs. all other behaviors and permuted data summarized in **D** are depicted in **E**. Panel **F** use LOO model building and evaluation to determine how models built and tested on sex specific populations perform within (male to male [M→M]; female to female [F→F]; solid lines) and across sexes (male to female [M→F]; female to male [F→M]; dashed lines).

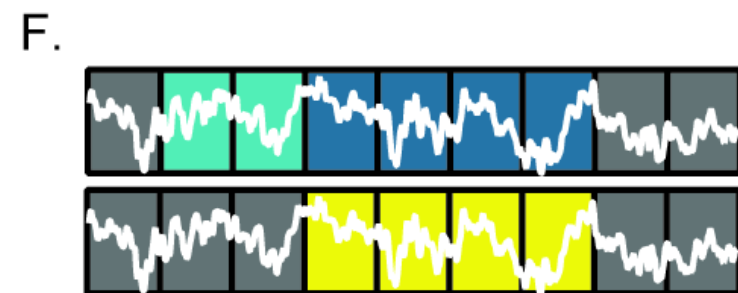
Figure 3. Local field potentials (LFPs) recorded in the nucleus accumbens (NAc) shell can predict sweet-fat food (SF) or 10% ethanol (EtOH) consumption versus all other behavior more accurately as separate models than as a single general model. Panels **A-D** illustrates the outcomes of models built using the 80/20 approach and **E-F** the leave one out (LOO) approach. Panels **A** and **E** illustrate the performance of models predicting SF (green) or EtOH (blue) consumption versus all other behavior using only LFP features from the bilateral NAc shell. These receiver operator characteristic (ROC) curves illustrate how the true positive rate (TPR) varies in relation to the false positive rate (FPR). The average area under the ROC curve (AUROC) is shown \pm 95% confidence intervals. Panels **B** and **F** show how the models perform when we apply them to the other dataset (e.g., built on feeding data and tested on drinking data [feed → drink]). Panels **C** and **G** show the performance of generalized (gen) models built and tested on a combination of the feeding and drinking datasets (dashed teal curve). The blue (drinking) and green (feeding) curves illustrate how the general model performs on those specific types of data. Panels **D** and **F** depict how each individual LFP feature performs

(AUROC) when we build and test models on each dataset separately. The sign of the AUROC value indicates the direction of feature change during consumption – if features change in the same way for both types of consumption they would be in quadrants I and III. The blue features (right delta power and left high gamma power) are the most important features in the generalized models.

Figure 4. Local field potentials (LFPs) recorded from rat medial pre-frontal cortex and ventral striatal regions are able to predict that a rat is about to consume sweet-fat food (SF) with greater accuracy than 10% ethanol (EtOH). Panels **A** and **D** illustrate model performance (area under the receiver operator characteristic curve; AUROC) predicting imminent consumption moving back through time from initiation of feeding (light green curve) or drinking (light blue curve). The black curves in **A** and **D** are the average performance of corresponding models built and tested on permutations of the real data. The horizontal green (**A**) and blue (**D**) bars at time zero indicate the AUROC of the corresponding consumption vs. not models. While there is clear information about imminent feeding that diminishes back through time (**A**), there is minimal information about imminent drinking (**D**). Panels **B** and **E** are examples of how single LFP features vary around intervals of eating SF (**B**) and drinking EtOH (**E**). Light green and light blue indicate feature values from 5 second bins prior to consumption, purple segments indicate data bins that straddle two behavior categories – the 5 second analytical window includes time in both behaviors – and black/grey indicates time after consumption interval. Solid black/grey lines indicate the average feature value during all other behaviors and dashed horizontal lines indicate average feature value during consumption. Panels **C** and **F** show the performance of individual LFP features (AUROC) and the direction of feature change in the corresponding consumption (y-axis) and pre-consumption (x-axis) models for feeding (**C**) and drinking (**F**).



- [Grey box] not consuming
- [Green box] consuming SF
- [Yellow box] pre-consumption SF
- [Purple box] consumption HC



- [Grey box] not consuming
- [Blue box] consuming EtOH
- [Cyan box] pre-consumption EtOH
- [Yellow box] consumption H₂O

model types

[Green box] vs [Grey box] [Purple box] consuming vs. not

[Yellow box] vs [Grey box] [Purple box] pre-consuming vs. not

consuming (EtOH or SF) vs. not

[Blue box] vs [Grey box] [Yellow box] [Cyan box] vs [Grey box] [Yellow box] [Grey box] vs [Grey box] [Yellow box] [Purple box]

